Journal of The Electrochemical Society, **150** (5) C362-C367 (2003)
0013-4651/2003/150(5)/C362/6/$7.00 © The Electrochemical Society, Inc.

Direct Copper Electrodeposition on TaN Barrier Layers

Aleksandar Radisic,[a,*,z] Yang Cao,[b,] Premratn Taephaisitphongse,[b] Alan C. West,[b,**] and Peter C. Searson[a,**]**

[a]*Department of Materials Science and Engineering, Johns Hopkins University, Baltimore, Maryland 21218, USA* [b]*Department of Chemical Engineering, Columbia University, New York, New York 10027, USA*

In this paper we report on nucleation and growth of copper onto TaN from sulfate, ethylenediaminetetraacetate, citrate, and fluoroborate solutions. The onset for copper deposition on TaN is shifted negative by 0.65 V to 1 V compared to deposition on Pt, depending on the solution chemistry. For all solutions, deposition occurs by three-dimensional island growth. The island density generally increases strongly with increasing overpotential and is also dependent on solution chemistry.
 [DOI: 10.1149/1.1565137]

Manuscript submitted April 25, 2002; revised manuscript received October 8, 2002. Available electronically April 3, 2003.

In current copper metallization technology,[1-3] copper is electrodeposited onto a barrier layer precovered by a thin copper seed layer deposited using physical vapor deposition (PVD) or chemical vapor deposition (CVD) techniques. As the feature sizes of trenches and vias continue to shrink, the ability to deposit a continuous and defect-free seed layer is becoming increasingly difficult. Furthermore, with feature sizes decreasing below 100 nm, the seed layer will become a significant fraction of the metallization. As a result, strategies for the direct deposition of copper onto the barrier layer are being explored.

In this paper, we report on electrodeposition of copper onto TaN barrier layers from the sulfate, fluoroborate, ethylenediaminetetraacetate (EDTA), and citrate solutions. These solutions include complexing and noncomplexing agents and span a wide range of pH values. Copper sulfate solutions (Ref. 4-12 and references therein) are currently used in copper metallization technology. These solutions usually contain additives such as polyethylene glycol (PEG) and chloride ions, which co-adsorb on the copper surface and decrease the rate of deposition.[11,12] The addition of additives such as bis(3-sulfopropyl) disulfide (SPS) results in enhanced deposition rates at the bottom of features such as trenches or vias, leading to void- free deposits.[3] Copper deposition from sulfate solutions on copper seed layers has been studied in detail, and a number of models for deposition into patterned structures have been reported in the literature.[4-10]

Copper fluoroborate solutions[13,14] allow the use of high deposition current densities. Disproportionation of fluoroborate results in the formation of hydrofluoric acid, which can minimize the formation of surface oxide layers. In previous work, we have reported on the nucleation and growth of copper on TiN[14] from fluoroborate solution. Copper EDTA solutions are commonly used in electroless copper deposition. However, EDTA solutions have been explored for electrodeposition of copper on TiN.[15] Citrate solutions[16] are attractive since the citrate ion can function as a brightening, leveling, and buffering agent (Ref. 17 and references therein). Citrate solutions are of technological interest since they have low toxicity, however, their stability is a major disadvantage. An important application of citrate solutions is the electrodeposition of copper-nickel alloys.[17]

Experimental

All experiments on nonpatterned wafers were performed on a 50 nm thick TaN diffusion barrier layer deposited on a thermal oxide supplied by a chip manufacturer. The composition of the barrier layer was $Ta_{1.73}N$, determined by Auger electron spectroscopy (AES). The resistivity of the film was 250 $\mu\Omega$ cm.

Four solutions were investigated, copper sulfate, copper EDTA, copper citrate, and copper fluoroborate. The copper sulfate solution (pH 0.1) contained 0.05 M $CuSO_4 \cdot 5H_2O$ (Aldrich Chemical Co., Inc.), 0.375 M H_2SO_4 (J. T. Baker), 1.84×10^{-5} M (62.5 mg L^{-1}) polyethylene glycol (PEG) (average M_n 3400, Aldrich Chemical Co., Inc.), 2.93×10^{-4} M (10.4 mg L^{-1}) Cl^- (J. T. Baker), and 2.82×10^{-6} M (1 mg L^{-1}) bis(3-sulfopropyl) disulfide (SPS Raschig Corp.). The copper fluoroborate solution contained 0.05 M $CuCO_3 \cdot Cu(OH)_2$ (Aldrich Chemical Co., Inc.) + 0.32 M H_3BO_3 (J. T. Baker) + 0.36 M HBF_4 (48 wt %, Aldrich Chemical Co., Inc.) (pH 1). The copper citrate solution contained either 0.05 M $CuSO_4 \cdot 5H_2O$ + 0.5 M citric acid [$HOCCOOH(CH_2COOH)_2$] (EM Science) or 0.025 M $CuSO_4 \cdot 5H_2O$ + 0.25 M citric acid, and 0.93 M Na_2SO_4 (J. T. Baker) with the pH adjusted to 3.1. In some experiments the pH was adjusted to the range 2.5-13.2. The basic composition of the copper EDTA solution was 0.05 M $CuSO_4 \cdot 5H_2O$ + 0.1 M EDTA (J. T. Baker) with the pH adjusted to 13.5 using NaOH.[15] Solutions containing both lower (0.035 M $CuSO_4 \cdot 5H_2O$ + 0.07 M EDTA) and higher copper concentration (0.24 M $CuSO_4 \cdot 5H_2O$ + 0.48 M EDTA) were also evaluated. In some experiments, the pH of the copper EDTA solution was adjusted to the range 9.5 to 13.8.

Cyclic voltammetry was performed on platinum foils and TaN films in a three-electrode cell. A platinum mesh was used as a counter electrode, and a Ag/AgCl (3 M NaCl) electrode (0.22 V *vs.* NHE) served as a reference electrode. Unless otherwise stated, the working electrode area was 0.385 cm^2 with an electrical contact around the perimeter of the electrode. All samples were immersed in 70% HNO_3 (J. T. Baker) for 30 s and then rinsed with distilled, deionized water prior to each experiment.[18,19] Atomic force microscopy (AFM) revealed no change in surface roughness or morphology after this precleaning treatment. We note that similar results were obtained after precleaning samples in 1-2 vol % HF (Alfa Aesar).

The influence of the sheet resistance on the density of copper islands was studied using constant current deposition experiments on rectangular samples about 2-2.5 cm long and 1.15 cm wide. Electrical contact was made to one end of the rectangle, and the sample was immersed 1.5-2.0 cm into the solution. A copper bar (99.99% Johnson- Matthey) served as a counter electrode.

All electrochemical measurements were performed using EG&G PAR 273/273A potentiostat/galvanostat. The films were examined by JEOL 5600 and JEOL 6700F scanning electron microscopes (SEMs).

Results and Discussion

Figure 1 shows cyclic voltammograms for Pt and TaN in copper sulfate (pH 0.1), fluoroborate (pH 1), citrate (pH 3.1), and EDTA (pH 13.5) solutions.

Voltammograms for copper deposition on Pt from sulfate, fluoroborate, citrate, and EDTA solution exhibited similar features. The

* Electrochemical Society Student Member.
** Electrochemical Society Active Member.
z E-mail: aradisi1@jhem.jhu.edu

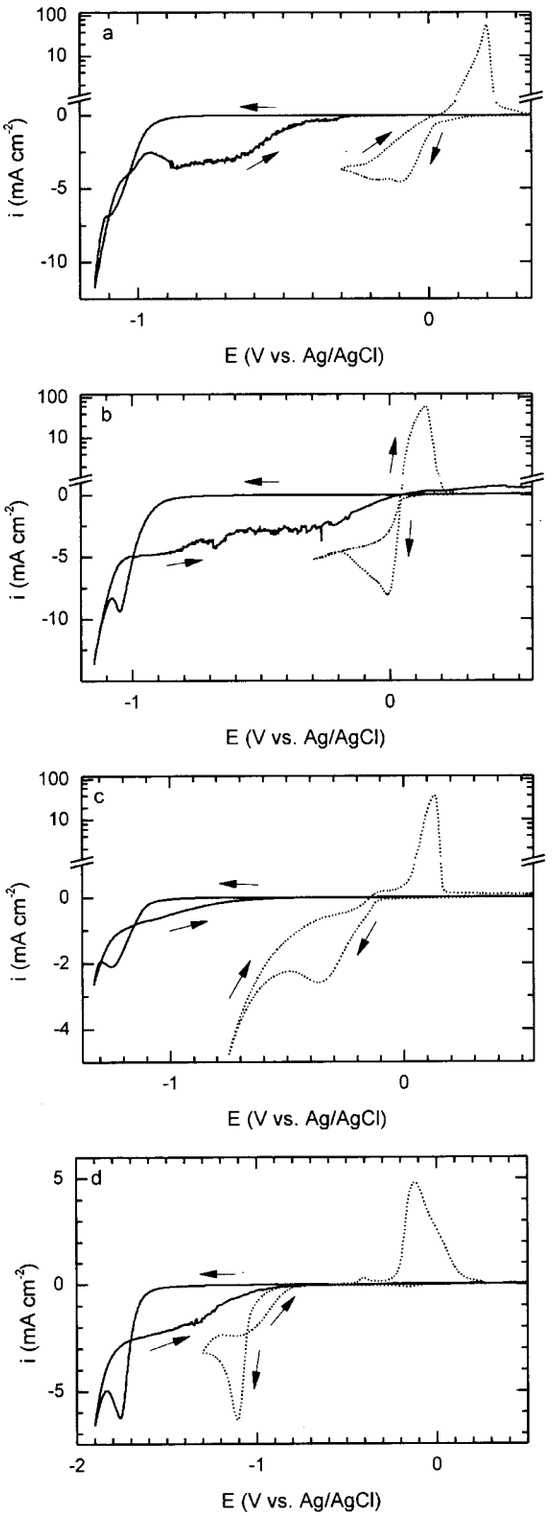

Figure 1. Cyclic voltammograms for copper deposition on platinum (dotted line) and TaN (solid line) diffusion barrier layer from: (a) 0.05 M $CuSO_4 \cdot 5H_2O$, 0.375 M H_2SO_4, 1.84×10^{-5} M (62.5 mg L^{-1}) PEG, 2.93×10^{-4} M (10.4 mg L^{-1}) Cl^-, and 2.82×10^{-6} M (1 mg L^{-1}) bis(3-sulfopropyl) disulfide (SPS) (pH 0.1), (b) 0.05 M $CuCO_3 \cdot Cu(OH)_2$, 0.32 M H_3BO_3, and 0.36 M HBF_4 (pH 1), (c) 0.05 M $CuSO_4 \cdot 5H_2O$, 0.5 M $HOCCOOH(CH_2COOH)_2$, 0.93 M Na_2SO_4 (pH 3.1), and d) 0.05 M $CuSO_4 \cdot 5H_2O$, 0.1 M EDTA (pH 13.5) solutions. For clarity, we introduced breaks in our plots at +1 mA cm^2 and plotted anodic peaks in logarithmic scale.

onset of copper deposition is followed by a characteristic peak associated with nucleation and diffusion-limited growth.[20] The copper deposition peaks were all in the range of 3-7 mA cm^{-2}. The potential of the peak was 0 V in fluoroborate, −0.1 V in sulfate, −0.35 V in citrate, and −1.1 V in EDTA. Note that the peak for the strongly complexing EDTA solution is shifted significantly compared to the other solutions. In the reverse scan, a diffusion-limited deposition current is followed by a stripping peak. For sulfate, fluoroborate, and citrate solutions stripping was fast with current densities in the range 40 to 60 mA cm^{-2}, about an order of magnitude larger than the deposition peak. The stripping peak in the EDTA solution was about 4.9 mA cm^{-2} at −0.1 V and was broad with a shoulder at 0 V, due to the formation of copper oxide.

Cyclic voltammograms for copper deposition on TaN were significantly different from those on Pt. The copper deposition peak is shifted more negative by 1 V for the case of sulfate and fluoroborate, 0.9 V for citrate, and 0.65 V for EDTA solutions. The shift in the deposition peak is related to the large nucleation overpotential on TaN. The copper deposition peak was immediately followed by hydrogen evolution, indicating that the copper clusters catalyze the hydrogen evolution reaction. For the case of voltammograms in sulfate and fluoroborate solutions, current fluctuations in the reverse scan were associated with the appearance of cracks in the deposited films. In sulfate solution, the copper deposition current becomes zero at about −0.25 V, several hundred millivolts negative of the zero current potential on Pt. Since the onset for nucleation and growth on TaN occurs at about −0.9 V, the fact that deposition stops at −0.25 V indicates that the copper film is delaminated during the reverse scan. No stripping peaks were observed in voltammograms for any of the solutions indicating that the copper film becomes electrically isolated from the TaN substrate during the reverse scan.

The kinetics of nucleation and growth were studied by analyzing deposition transients.[20] In these experiments, the potential was stepped from a potential where no deposition is observed, typically 100 mV negative to the open circuit potential, to potentials in the region of the bulk deposition peak, as determined from the cyclic voltammograms. Figure 2 shows current transients for copper deposition from 50 mM copper sulfate, fluoroborate, citrate, and EDTA solutions on TaN. The transients were characterized by an initial increase in current density due to nucleation and growth of three-dimensional (3D) copper clusters. At longer times the current decreased due to the transition from 3D to 1D growth. The current transients were replotted in dimensionless form and compared to the growth laws[21,22] for instantaneous and progressive nucleation followed by diffusion-limited 3D growth.

Figure 3 shows the current transients recorded at the potential of the deposition peak, for copper sulfate, fluoroborate, citrate, and EDTA solutions, in dimensionless form. Deposition from copper sulfate solution (Fig. 3a) initially follows the model for instantaneous nucleation followed by 3D diffusion-limited growth. At longer times, the deposition current density was larger than predicted by the model. This effect is often observed for systems where the onset of hydrogen evolution is close to the deposition peak;[13] the hydrogen evolution reaction is catalyzed by the deposition of the metal clusters leading to an additional contribution to the current. Copper deposition from copper fluoroborate (Fig. 3b) was not consistent with the model for nucleation followed by 3D diffusion-limited growth. The origin of the two peaks in the reduced current plot may be related to renucleation. The deposition current for copper citrate (Fig. 3c) is initially larger than predicted by the model for instantaneous nucleation followed by 3D diffusion-limited growth, whereas at longer times the agreement is excellent indicating that at long times growth is controlled by a one-dimensional diffusion field. For the case of deposition from copper EDTA solution (Fig. 3d), at short times the deposition transients follow the model for progressive nucleation followed by 3D diffusion-limited growth, but at longer times the reduced current density is much lower than predicted by the model.

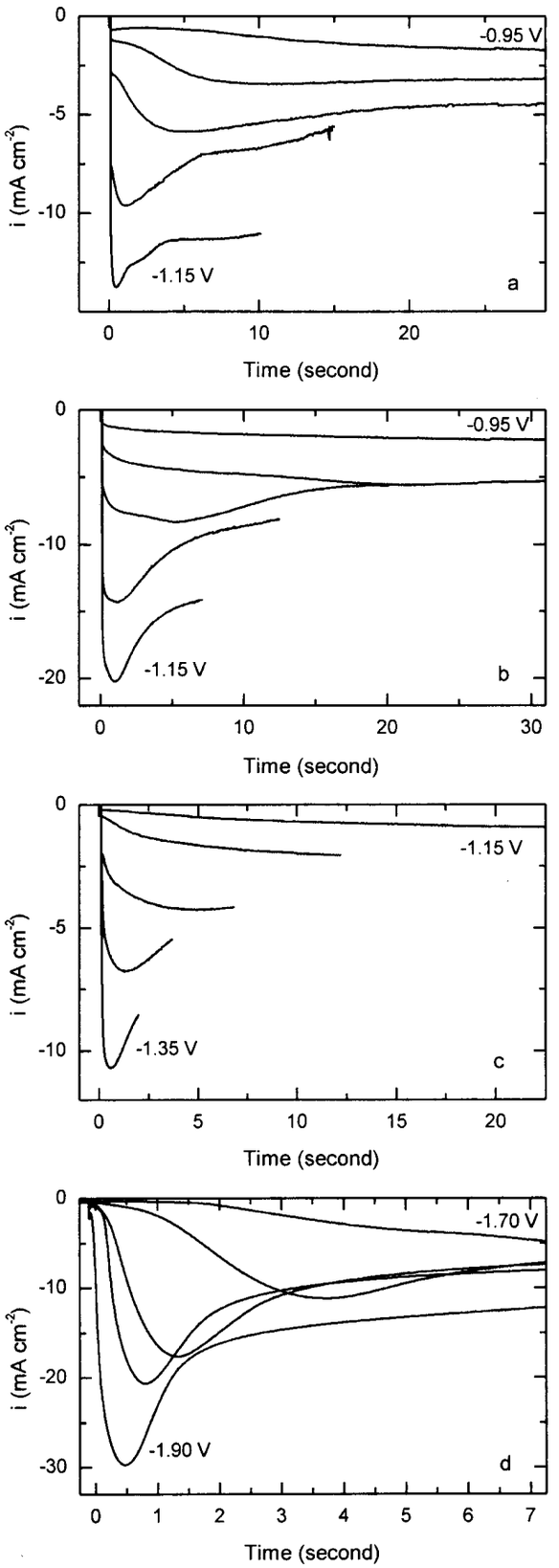

Figure 2. Current transients for copper deposition on TaN from: (a) 50 mM copper sulfate (pH 0.1) at −0.95, −1.0, −1.05, −1.1, and −1.15 V, (b) fluoroborate (pH 1) at −0.95, −1.0, −1.05, −1.1, and −1.15, (c) citrate (pH 3.1) at −1.15, −1.20, −1.25, −1.30, and −1.35 V, and (d) EDTA (pH 13.5) at −1.70, −1.75, −1.80, −1.85, and −1.90 V.

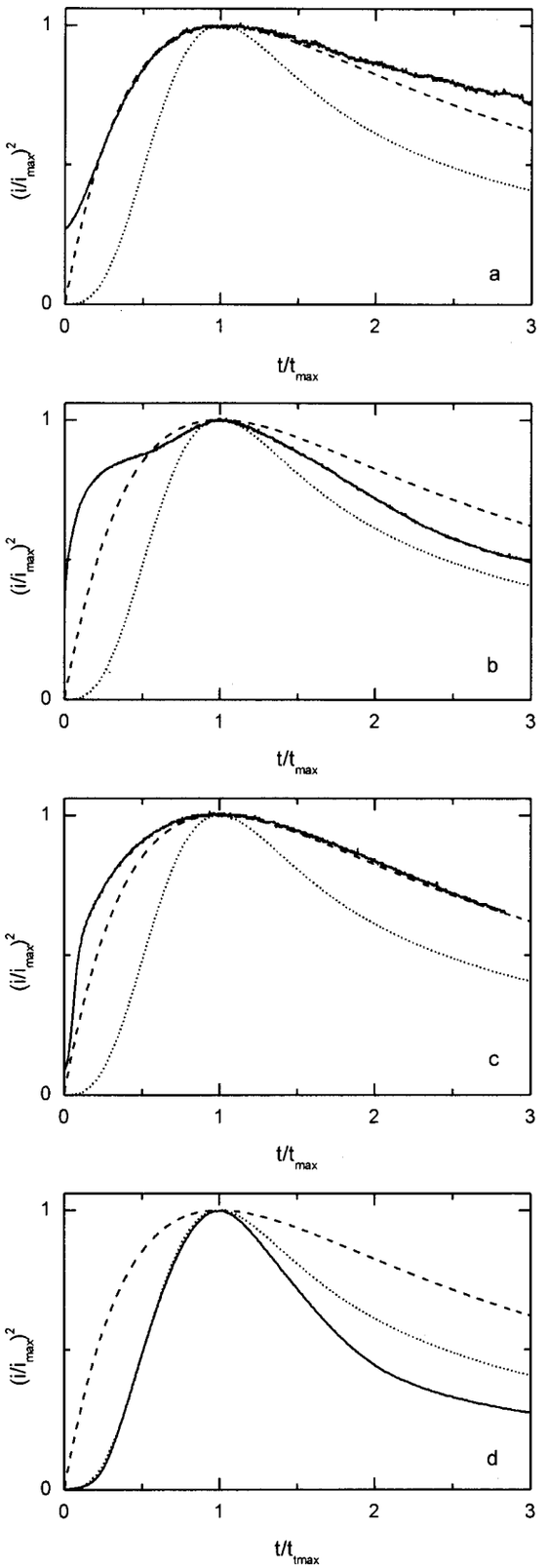

Figure 3. Normalized current transients (solid line) for copper deposition on TaN from: (a) 50 mM copper-sulfate (pH 0.1) at −1.05 V, (b) fluoroborate (pH 1) at −1.05 V, (c) citrate (pH 3.1) at −1.25 V, and (d) EDTA (pH 13.5) at −1.75 V. Also plotted are transients obtained using models for instantaneous nucleation followed by 3D diffusion-limited growth (dashed line) and for progressive nucleation followed by 3D diffusion-limited growth (dotted line).

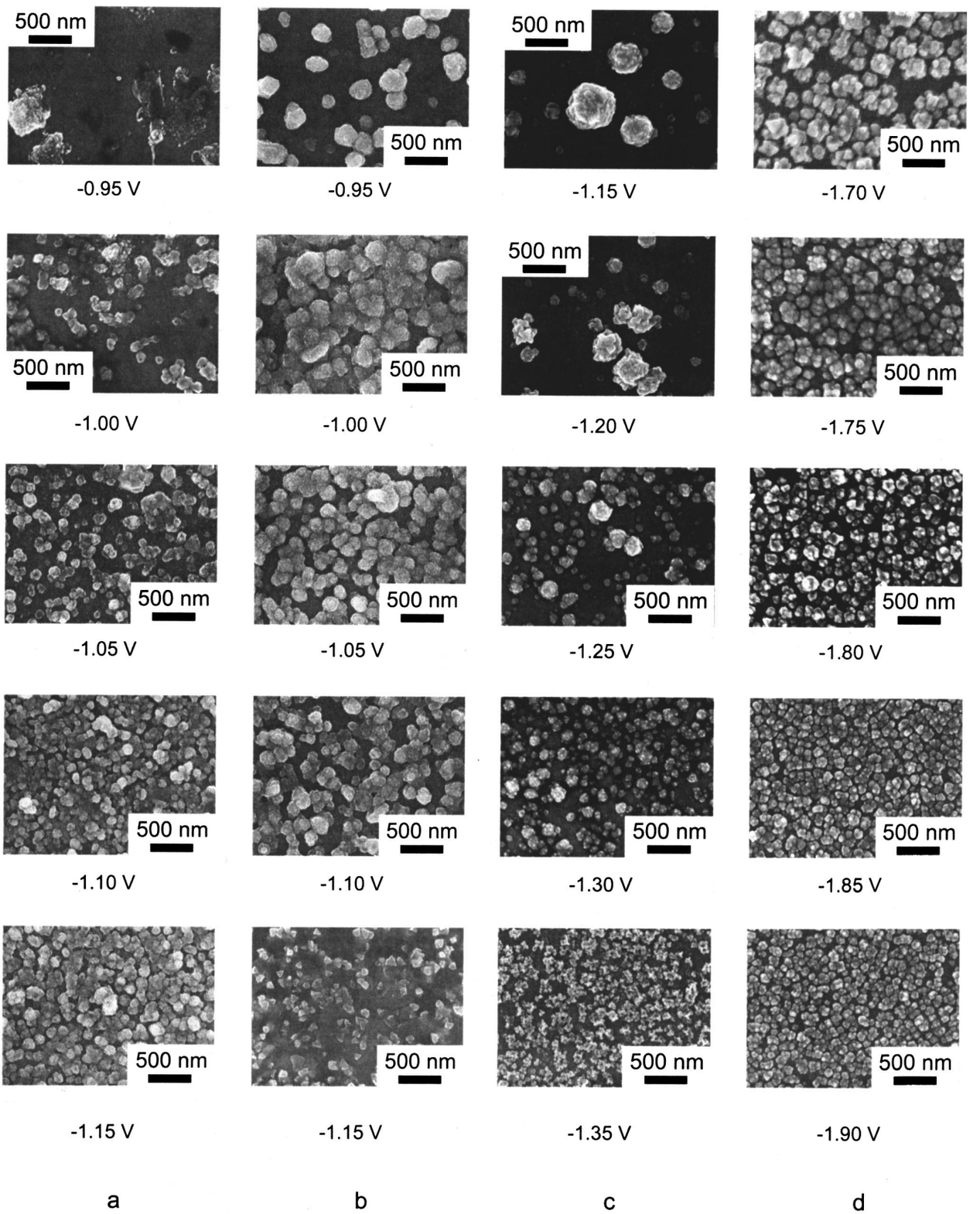

Figure 4. SEM images of copper clusters deposited from (a) 50 mM copper sulfate (pH 0.1) at −0.95, −1.0, −1.05, −1.1, and −1.15, (b) fluoroborate (pH 1) at −0.95, −1.0, −1.05, −1.1, and −1.15, (c) citrate (pH 3.1) at −1.15, −1.20, −1.25, −1.30, and −1.35, and (d) EDTA (pH 13.5) at −1.70, −1.75, −1.80, −1.85, and −1.90 V.

The potential dependence of the nucleus density was determined from SEM images. Figure 4 shows series of images of copper clustersobtained from copper sulfate, fluoroborate, citrate, and EDTA-based solutions at different potentials. All images were re-

corded at 1.5 mm radial distance from the perimeter of the electrode. In all cases the clusters were randomly distributed on the surface. Copper clusters deposited from sulfate solution were similar in diameter, indicating that nucleation is fast in comparison to growth and consistent with the normalized deposition transient shown in Fig. 3a. Clusters deposited from the citrate solution exhibited a distribution of sizes characteristic of progressive nucleation, even though reduced parameter plots suggested processes closer to the model for instantaneous nucleation. Copper clusters deposited from EDTA solution also exhibited a broad distribution, consistent with the rising part of the normalized deposition transient and the model for progressive nucleation followed by 3D diffusion-limited growth.

At the potentials of the bulk deposition peak, −1.05 V for sulfate and fluoroborate, −1.25 V for citrate, and −1.75 V for EDTA solution, the highest cluster density was obtained for the copper EDTA solution. Figure 5 shows the potential dependence of the cluster density in fluoroborate, citrate, and EDTA solutions.

The cluster density in fluoroborate solution increases sharply with potential and appears to saturate at more negative potentials. Similar results have been reported for copper deposition from fluoroborate solution on TiN.[13] The copper cluster density in citrate and EDTA solutions is exponentially dependent on potentials with inverse slopes of 150 and 250 mV/dec, respectively. In classical models for electrodeposition, an increase in the cluster density with overpotential is related to a distribution of activation energies associated with nucleation sites.[23] From Fig. 5 it is seen that cluster densities in excess of 10^{10} cm^{-2} can be obtained in the potential region prior to dominant hydrogen evolution for EDTA and citrate solution. However, the results from Fig. 5 indicate that solution chemistry has a strong influence on cluster density.

Electrochemical deposition on diffusion barrier materials generally occurs by 3D island growth. Consequently, high nucleus densities are essential in designing processes for thin-film deposition since the critical film thickness for island coalescence, d_{crit}, is directly related to the island density, *N*. For hemispherical clusters, $d_{crit} = 0.5\ N^{-1/2}$. From this expression it is clear that cluster densities in excess of 10^{11} cm^{-2} are necessary to achieve coalescence at a film thickness of 10 nm. Figure 5 shows that the potential is an important parameter in manipulating the island density and hence in controlling the critical thickness for coalescence. Furthermore, Fig. 5 shows that the strongly cluster density is the deposition dependent on solution chemistry. The strong exponential dependence of island density on potential for EDTA and citrate solutions suggests a similar mechanism for island formation. From Fig. 1 it is evident that the shift in the curves is related to the slower kinetics for the EDTA solutions.

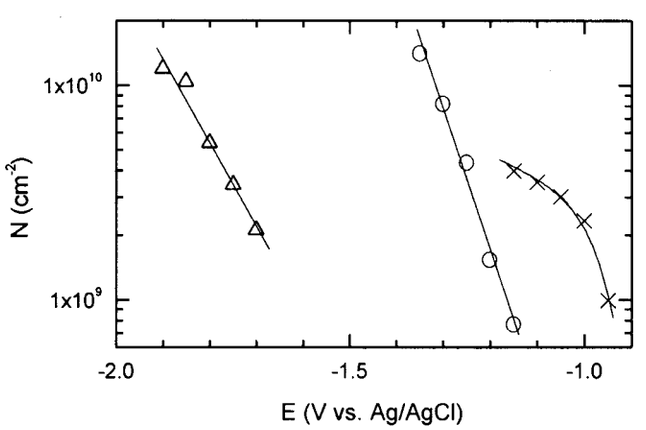

Figure 5. Potential dependence of copper cluster density for solutions containing: (×) 0.05 M $CuCO_3 \cdot Cu(OH)_2$, 0.32 M H_3BO_3, 0.36 M HBF_4 (pH 1); (○) 0.05 M $CuSO_4 \cdot 5H_2O$, 0.5 M $HOCCOOH(CH_2COOH)_2$, 0.93 M Na_2SO_4 (pH 3.1); and (△) 0.05 M $CuSO_4 \cdot 5H_2O$, 0.1 M EDTA (pH 13.5).

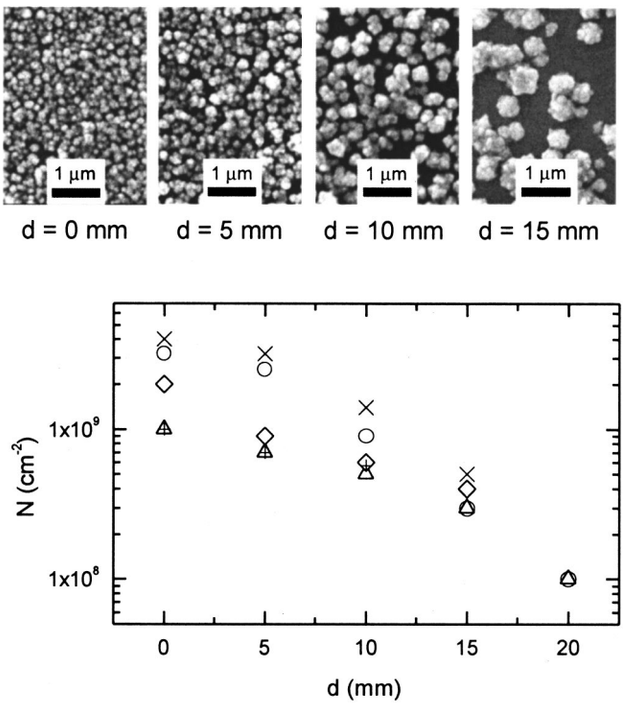

Figure 6. Copper cluster density *vs.* distance from the electrical contact. Copper was deposited from solution containing 0.035 M $CuSO_4 \cdot 5H_2O$ and 0.07 M EDTA (pH 13.4) at (+) 1 mA cm^{-2} for 400 s, at (○) 3.1 mA cm^{-2} for 150 s, and at (×) 4.0 mA cm^{-2} for 10 s, and a solution containing 0.025 M $CuSO_4 \cdot 5H_2O$ + 0.25 M $HOCCOOH(CH_2COOH)_2$ + 0.93 M Na_2+SO_4 (pH 3.1) at (△) 1 mA cm^{-2} for 600 s, and at (◇) 5.0 mA cm^{-2} for 150.

Based on these results we deposited copper thin films on TaN using a two-step potentiostatic technique. The first step involved a short potential pulse, close to the onset of hydrogen evolution in order to obtain a high cluster density, while in the second step a more positive potential was applied to grow the clusters. By using this approach we were able to grow bright, continuous copper films. Many thin film samples passed a qualitative tape test, *i.e.*, no observable copper was removed from the sample after the tape is removed. However, the copper was removed by rubbing the sample.

The quality and adhesion of the copper films was also dependent on the solution pH. For the EDTA solution, the pH was varied from 9.5 to 13.8. In general, the best results were obtained in the pH range between 13 and 13.5.[15] For citrate solutions, films were deposited in the pH range, from 2.5 to 13.2. In this solution, the best results were obtained from pH 2.5 to 5.0. At higher pH values (>5), adhesion between the deposited copper film and TaN substrate was poor, and the solutions were unstable with slow precipitation. For both citrate and EDTA solutions, the optimum pH range corresponds to the regime where CuOHL (where L is the ligand) is the dominant species.[16]

The influence of the sheet resistance of the TaN film on nucleation and growth was determined by performing experiments on rectangular samples with an ohmic contact at one end. Copper was deposited from EDTA and citrate solutions onto 50 nm thick TaN barrier layers (resistivity 250 μΩ cm) at a constant current of 1 to 5 mA cm^{-2}. In all cases, a continuous color variation along the length of the sample indicated the nonuniformity of the deposited film with copper preferentially deposited closer to the electrical contact. Figure 6 shows a plot of the density of copper clusters, deposited onto TaN from a solution containing 0.035 M $CuSO_4 \cdot 5H_2O$ + 0.07 M EDTA (pH 13.4), and solution containing 0.025 M $CuSO_4 \cdot 5H_2O$ + 0.25 M citrate acid +0.93 M Na_2SO_4 (pH 3.1) *vs.* distance. Also

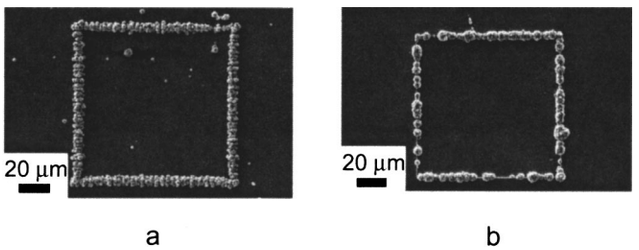

Figure 7. SEM images of copper deposition from stagnant solutions of (a) 0.025 M $CuSO_4 \cdot 5H_2O$, 0.25 M $HOCCOOH(CH_2COOH)_2$, and 0.93 M Na_2SO_4 (pH 3.1), and (b) 0.035 M $CuSO_4 \cdot 5H_2O$ and 0.07 M EDTA (pH 13.4) onto TaN-patterned wafers.

shown in Fig. 6 are SEM images of copper clusters as a function of distance from the contact. Note that cluster density is the same order of magnitude as the constant potential measurements (Fig. 5). The potential difference between the point on the sample closest to the electrical contact and the point furthest away from it was estimated to be between 50-100 mV using models for deposition on resistive substrates.[24,25]

We have also explored copper deposition onto patterned diffusion barrier layers. Figure 7 shows copper clusters deposited onto patterned TaN from citrate and EDTA based copper solutions. In both cases copper was deposited at a constant current density of 1 mA cm^{-2} for 600 s. From this figure it can be seen that copper clusters were deposited preferentially on the sidewalls of a feature approximately 1 μm deep. Similar results were obtained for smaller features with other geometries. This result shows that geometry also plays a key role in determining the spatial distribution of nuclei at the surface.

Conclusions

Direct copper electrodeposition on TaN diffusion barrier layers is characterized by Volmer-Webber (3D) island growth. The nucleation overpotential is between 0.65 to 1 V larger on TaN than on Pt. For citrate and EDTA solutions the cluster density increased exponentially with more negative potentials. For fluoroborate solutions the cluster density increased and then saturated at more negative potentials. Cluster densities in excess of 10^{10} cm^{-2} were obtained by applying potential steps close to the onset of hydrogen evolution. Bright, continuous, copper films were obtained by using a double potential step method.

Acknowledgments

The authors acknowledge support from the Semiconductor Research Corporation (Task ID 448.049 and Task ID 448.050) and the National Science Foundation (grant no. CTS-0122909).

Johns Hopkins University assisted in meeting the publication costs of this article.

References

1. D. Edelstein, J. Heidenreich, R. Goldblatt, W. Cote, C. Uzoh, N. Lustig, P. Roper, T. McDevitt, W. Motsfiff, A. Simon, J. Dukovic, R. Wachnik, H. Rathore, R. Shultz, L. Su, S. Luce, and J. Slattery, *Tech. Dig. - Int. Electron Devices Meet.*, **1997**, 773.
2. D. C. Edelstein, G. A. Sai-Halasz, and Y. J. Mii, *IBM J. Res. Dev.*, **39**, 383 (1995).
3. P. C. Andricacos, C. Uzoh, J. O. Dukovic, J. Horkans, and H. Deligianni, *IBM J. Res. Dev.*, **42**, 567 (1998).
4. J. J. Kelly and A. C. West, *Electrochem. Solid-State Lett.*, **2**, 561 (1999).
5. J. J. Kelly, C. Tian, and A. C. West, *J. Electrochem. Soc.*, **146**, 2540 (1999).
6. A. C. West, *J. Electrochem. Soc.*, **147**, 227 (2000).
7. Y. Cao, P. Taephaisitphongse, R. Chalupa, and A. C. West, *J. Electrochem. Soc.*, **148**, C466 (2001).
8. T. P. Moffat, J. E. Bonevich, W. H. Huber, A. Stanishevsky, D. R. Kelly, G. R. Stafford, and D. Josell, *J. Electrochem. Soc.*, **147**, 4524 (2000).
9. T. P. Moffat, D. Wheeler, W. H. Huber, and D. Josell, *Electrochem. Solid-State Lett.*, **4**, C26 (2001).
10. W. Plieth, *Electrochim. Acta*, **37**, 2115 (1992).
11. M. R. Hill and G. T. Rogers, *J. Electroanal. Chem.*, **86**, 179 (1978).
12. J. P. Healy and D. Pletcher, *J. Electroanal. Chem.*, **338**, 155 (1992).
13. G. Oskam, P. M. Vereecken, and P. C. Searson, *J. Electrochem. Soc.*, **146**, 1436 (1999).
14. A. Sato and R. Barauskas, *Metal Finishing, Guidebook and Directory Issue*, p. 230, Elsevier, New York (1997).
15. T. L. Gilton, M. E. Tuttle, and D. A. Cathey, US Pat. 5,151,168 (1992).
16. C. Henninot, C. Vallieres, S. Rode, and M. Matlosz, *Electrochemical Technology Applications in Electronics III*, L. T. Romankiw, T. Osaka, Y. Yarnazaki, and C. Madore, Editors, PV 99-34, p. 333, The Electrochemical Society Proceeding Series, Pennington, NJ (2000).
17. T. A. Green, A. E. Russell, and S. Roy, *J. Electrochem. Soc.*, **145**, 875 (1998).
18. W.-T. Tseng, C.-H. Lo, and S.-C. Lee, *J. Electrochem. Soc.*, **148**, C327 (2001).
19. W.-T. Tseng, C.-H. Lo, and S.-C. Lee, *J. Electrochem. Soc.*, **148**, C333 (2001).
20. Southampton Electrochemistry Group, *Instrumental Methods in Electrochemistry*, Ellis Harwood, Ltd., Chichester, UK (1985).
21. G. Gunawardena, G. J. Hills, I. Montenegro, and B. R. Scharifker, *J. Electroanal. Chem.*, **138**, 225 (1982).
22. B. R. Scharifker and G. J. Hills, *Electrochim. Acta*, **28**, 879 (1983).
23. E. Budevski, G. Staikov, and W. J. Lorentz, *Electrochemical Phase Formation and Growth*, VCH, New York (1996).
24. M. Matlosz, P.-H. Vallotton, A. C. West, and D. Landoldt, *J. Electrochem. Soc.*, **139**, 752 (1992).
25. P. Desprez, M. Matlosz, J. D. Yang, and A. C. West, *J. Electrochem. Soc.*, **145**, 165 (1998).